

## ARTICLES

# A nuclear receptor-like pathway regulating multidrug resistance in fungi

Jitendra K. Thakur<sup>1,2\*</sup>, Haribabu Arthanari<sup>3\*</sup>, Fajun Yang<sup>1,2\*</sup>, Shih-Jung Pan<sup>4</sup>, Xiaochun Fan<sup>3</sup>, Julia Breger<sup>5</sup>, Dominique P. Frueh<sup>3</sup>, Kailash Gulshan<sup>6</sup>, Darrick K. Li<sup>1</sup>, Eleftherios Mylonakis<sup>5</sup>, Kevin Struhl<sup>3</sup>, W. Scott Moye-Rowley<sup>6</sup>, Brendan P. Cormack<sup>4</sup>, Gerhard Wagner<sup>3</sup> & Anders M. Näär<sup>1,2</sup>

**Multidrug resistance (MDR) is a serious complication during treatment of opportunistic fungal infections that frequently afflict immunocompromised individuals, such as transplant recipients and cancer patients undergoing cytotoxic chemotherapy. Improved knowledge of the molecular pathways controlling MDR in pathogenic fungi should facilitate the development of novel therapies to combat these intransigent infections. MDR is often caused by upregulation of drug efflux pumps by members of the fungal zinc-cluster transcription-factor family (for example Pdr1p orthologues). However, the molecular mechanisms are poorly understood. Here we show that Pdr1p family members in *Saccharomyces cerevisiae* and the human pathogen *Candida glabrata* directly bind to structurally diverse drugs and xenobiotics, resulting in stimulated expression of drug efflux pumps and induction of MDR. Notably, this is mechanistically similar to regulation of MDR in vertebrates by the PXR nuclear receptor, revealing an unexpected functional analogy of fungal and metazoan regulators of MDR. We have also uncovered a critical and specific role of the Gal11p/MED15 subunit of the Mediator co-activator and its activator-targeted KIX domain in antifungal/xenobiotic-dependent regulation of MDR. This detailed mechanistic understanding of a fungal nuclear receptor-like gene regulatory pathway provides novel therapeutic targets for the treatment of multidrug-resistant fungal infections.**

Pathogenic fungi, especially *Candida* species, have emerged as important and prevalent opportunistic infections in individuals with compromised immunity, including those suffering from AIDS, cancer patients treated with chemotherapy, transplant recipients on immunosuppressive drugs and patients with advanced diabetes<sup>1,2</sup>. *Candida* species now account for 8–9% of all blood stream infections, with crude mortality rates of 40%<sup>3,4</sup>. Significantly, both intrinsic and acquired MDR is an important complication of fungal infections<sup>5</sup>. *C. glabrata*, which exhibits strong MDR, is emerging as a clinically important fungal pathogen, accounting, for example, for 20–24% of *Candida* blood stream infections in the USA<sup>1,3</sup>. There is thus an urgent need to elucidate the mechanisms underpinning MDR in pathogenic fungi to develop novel antifungal treatments. MDR in fungi is caused by the overexpression of membrane-spanning efflux pumps (for example the ATP-binding cassette (ABC) family of transporters), resulting in the expulsion of various structurally unrelated molecules<sup>6</sup>. Studies in *S. cerevisiae* have shown that the zinc-cluster transcription factor Pdr1p and the paralogue Pdr3p together confer resistance to several drugs and toxins through transcriptional activation of ABC transporter genes and members of the major facilitator superfamily of drug efflux pumps, including Pdr5p, Ssq2p and Yor1p, as well as phospholipid-transfer proteins such as Pdr16p<sup>7–15</sup>. Several studies recently reported increased expression of drug efflux pumps in yeast in response to different xenobiotics, and demonstrated a requirement for Pdr1p/Pdr3p in this response<sup>16–20</sup>, although the xenobiotic signalling pathway has not been elucidated. *C. glabrata* is evolutionarily closely related to *S. cerevisiae*, and recent studies have identified a Pdr1p orthologue (CgPdr1p) in *C. glabrata* that

regulates drug efflux pumps and controls MDR in this pathogen<sup>21–23</sup>. Increased knowledge of the mechanistic basis of CgPdr1p function in regulating multidrug resistance in *C. glabrata* could allow the identification of new classes of drugs to combat MDR in these clinically challenging infections.

Interestingly, the mammalian nuclear receptor pregnane X receptor (PXR) upregulates transcription of ABC transporters as well as cytochrome P450 detoxification enzymes in response to direct binding to structurally diverse xenobiotics<sup>24,25</sup>. However, similar direct transcription signalling mechanisms to regulate MDR have not been documented in non-vertebrate eukaryotes.

Transcription activators recruit co-activators that facilitate gene activation<sup>26</sup>. The Mediator co-activator, first characterized in yeast, interacts with RNA polymerase II and is involved in many transcriptional regulatory pathways<sup>27</sup>. The co-activator requirements, including a possible role of the Mediator, for xenobiotic-dependent transactivation of the MDR programme by Pdr1p orthologues have not been determined. Identification of co-activator targets for Pdr1p orthologues could facilitate the development of novel anti-MDR agents that target the activator/co-activator interface.

We show here that the Pdr1p orthologues in *S. cerevisiae* and *C. glabrata* directly bind xenobiotics to activate genes encoding drug efflux pumps, and exhibit functional characteristics that are mechanistically similar to the vertebrate xenobiotic receptor PXR. Moreover, our results demonstrate an essential and specific role for the Mediator co-activator subunit Gal11p (also known as MED15) in xenobiotic-dependent gene activation and MDR in *S. cerevisiae* and *C. glabrata*. The activation domains of Pdr1p orthologues bind

<sup>1</sup>Massachusetts General Hospital Cancer Center, Charlestown, Massachusetts 02129, USA. <sup>2</sup>Department of Cell Biology, <sup>3</sup>Department of Biological Chemistry and Molecular Pharmacology, Harvard Medical School, Boston, Massachusetts 02115, USA. <sup>4</sup>Department of Molecular Biology and Genetics, Johns Hopkins School of Medicine, Baltimore, Maryland 21205, USA. <sup>5</sup>Division of Infectious Diseases, Massachusetts General Hospital, Boston, Massachusetts 02114, USA. <sup>6</sup>Department of Molecular Physiology and Biophysics, University of Iowa, Iowa City, Iowa 52242, USA.

\*These authors contributed equally to this work.

directly to a domain present in Gal11p that is structurally conserved with the activator-binding KIX domain found in the human ARC105/MED15 Mediator subunit and in vertebrate CBP/p300 acetyltransferases. Our results demonstrate that fungi harbour a nuclear receptor-like pathway controlling MDR, which could represent a novel therapeutic target for the treatment of MDR in pathogenic fungi such as *C. glabrata*.

### Pdr1p and Pdr3p are xenobiotic receptors

The expression of ATP-dependent drug efflux pumps (for example *PDR5*) and other Pdr1p/Pdr3p target genes (for example *PDR16*) in *S. cerevisiae* can be induced by chemically distinct drugs and xenobiotics, including the antifungal ketoconazole, the translation inhibitor cycloheximide and the classic PXR agonist rifampicin, in a Pdr1p/Pdr3p-dependent manner (Fig. 1a and data not shown). In contrast, the glucocorticoid receptor agonist dexamethasone was consistently a poor inducer of Pdr1p/Pdr3p-regulated genes (Fig. 1a). Because the mammalian nuclear receptor PXR controls MDR gene expression by direct binding to xenobiotics<sup>24,25</sup>, and based on the intriguing functional similarities of Pdr1p/Pdr3p to PXR, we tested whether Pdr1p and Pdr3p could also directly interact with xenobiotics to stimulate expression of their target genes. Importantly, immunopurified Pdr1p binds ketoconazole with a dissociation constant ( $K_D$ ) of about 39  $\mu\text{M}$ , similar to the range of binding affinities (mid-nanomolar to high micromolar) of ligands for mammalian PXR (Fig. 1b)<sup>24</sup>. Binding of radiolabelled ketoconazole to Pdr1p was effectively competed by unlabelled xenobiotics that activate Pdr1p/Pdr3p target genes *in vivo*, including rifampicin,

cycloheximide and ketoconazole itself (Fig. 1b, c). Similar results were obtained with the Pdr1p paralogue Pdr3p, consistent with its functional redundancy in gene expression assays with these xenobiotics (Supplementary Fig. 2a, b and data not shown). Deletion analysis revealed that a small region in Pdr1p (amino acids 352–543) carboxy (C)-terminal to the DNA-binding domain is sufficient for binding to ketoconazole (Fig. 1d and Supplementary Fig. 2c, d). A similar region in Pdr3p also mediates ketoconazole binding, supporting the notion of a discrete xenobiotic-binding domain (XBD) in this family of zinc-cluster transcription factors (Supplementary Fig. 2e, f). Nuclear receptors harbour autonomous ligand-binding domains and ligand-responsive activation domains located C-terminal to the zinc finger DNA-binding domain that can be transferred to heterologous DNA-binding domains. Fusion experiments to the yeast Gal4p DNA-binding domain (Gal4pDBD) identified a large C-terminal domain in Pdr1p (amino acids 352–1063), encompassing both the XBD and the C-terminal activation domain, as the minimal transferable xenobiotic-responsive transactivation domain (Fig. 1d and Supplementary Fig. 3a, b). These results demonstrate that yeast Pdr1p/Pdr3p activate transcription of target genes in response to direct binding to specific xenobiotics by a discrete transferable ligand-binding domain, which suggests that these critical transcription regulators of MDR in yeast function in a manner analogous to the vertebrate nuclear receptor PXR.

### Requirement for Gal11p in xenobiotic response and MDR

Next, we studied the transcriptional co-activator requirements for ligand-dependent gene activation by Pdr1p/Pdr3p. The Mediator co-activator plays critical roles in transcriptional activation, from yeast to human<sup>27</sup>. We therefore examined whether the Mediator is involved in Pdr1p/Pdr3p-dependent and xenobiotic-stimulated gene activation and MDR. Although deletion of most Mediator subunits caused few or modest effects on MDR, deletion of the gene encoding the Gal11p subunit resulted in striking sensitivity to several toxins/xenobiotics, including ketoconazole, cycloheximide and 4-nitroquinoline oxide (Fig. 2a and data not shown). Consistent with these findings, xenobiotic-dependent expression of the *PDR5* and *PDR16* genes was specifically and strongly decreased in the *GAL11* deletion strain, similar to that observed with the *PDR1/3* deletion strain (Fig. 2b and data not shown). Moreover, deletion of the Pdr1p/Pdr3p-responsive promoters from the *PDR5* and *SNQ2* genes by constitutively active Pdr1p and Pdr3p mutants isolated from multidrug-resistant yeast (Supplementary Fig. 4)<sup>9,28,29</sup>. Co-immunoprecipitation experiments showed that Myc<sub>6</sub>-Pdr1p interacts with Gal11p-Flag<sub>2</sub> in a xenobiotic-stimulated manner *in vivo* (Fig. 2c), and chromatin immunoprecipitation data indicate that Gal11p is specifically recruited to Pdr1p/Pdr3p target genes in a Pdr1p/Pdr3p-dependent fashion (Supplementary Fig. 5 and data not shown). These studies demonstrate that Gal11p is essential for xenobiotic-dependent gene activation and MDR mediated by Pdr1p/Pdr3p.

### Gal11p harbours an activator-binding KIX domain

Gal11p orthologues contain sequences in their amino termini that exhibit significant homology to the activator-binding KIX domain of the metazoan Mediator subunit ARC105/MED15 (Supplementary Fig. 6a)<sup>30,31</sup>. The KIX domain was first identified as an activator target in the histone acetyltransferases CBP/p300, mediating interactions with many metazoan transcription factors<sup>32</sup>. Based on the documented functional importance of the KIX domains in ARC105/MED15 and CBP/p300 in specific gene-activation pathways<sup>31,33–35</sup>, we attempted to identify activators in yeast that interact with the predicted Gal11p KIX domain. Remarkably, affinity chromatography of yeast whole-cell extract over the putative Gal11p KIX domain yielded a single specific band that was identified by mass spectrometry as Pdr1p (Supplementary Fig. 6b, c), demonstrating that Pdr1p interacts strongly with the putative Gal11p KIX domain.

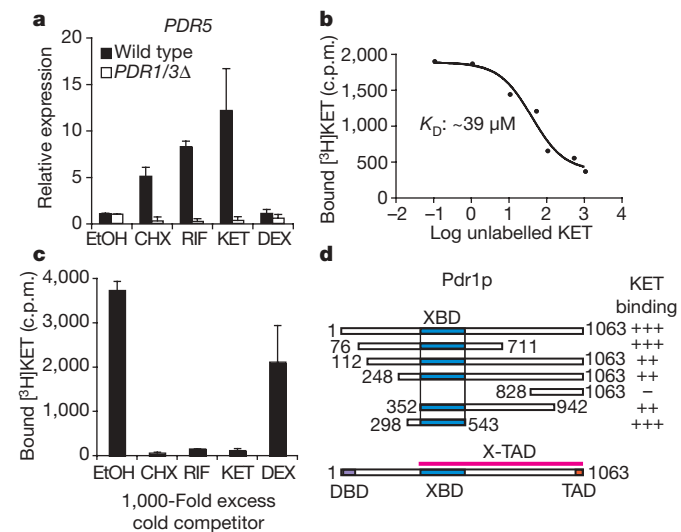


**Figure 1 | Pdr1p is a xenobiotic receptor.** **a**, Xenobiotic-induced transcription of the *PDR5* gene is dependent on Pdr1p/Pdr3p. Quantitative real-time RT-PCR reactions were performed in triplicate. Mean values from three independent experiments are shown; error bars, s.d. EtOH, ethanol, vehicle; CHX, cycloheximide; RIF, rifampicin; KET, ketoconazole; DEX, dexamethasone. **b**, Pdr1p directly binds to the antifungal ketoconazole. Cold ligand competition was used to determine the binding affinity of [<sup>3</sup>H]KET to Myc<sub>6</sub>-Pdr1p. [<sup>3</sup>H]KET (0.1  $\mu\text{M}$ ) was used for this experiment. Logarithmic concentration of unlabelled KET is displayed on the x axis. Mean values from triplicate samples are shown. The graph was generated using GraphPad Prism4. **c**, Cold competition assay reveals binding of various xenobiotics to Myc<sub>6</sub>-Pdr1p. Unlabelled xenobiotics were used for competition (x axis). The experiment was performed in triplicate. Mean values are shown; error bars, s.d. **d**, The xenobiotic-binding domain of Pdr1p. Glutathione-Sepharose beads with GST-Pdr1p protein fragments were used for direct binding assay using 0.1  $\mu\text{M}$  of [<sup>3</sup>H]KET. Symbols: +, binding; -, no binding. Lower cartoon shows positions of the DNA-binding domain (DBD), the xenobiotic-binding domain (XBD), the transactivation domain (TAD) and the xenobiotic-responsive transactivation domain (X-TAD).

We have also found that the putative Gal11p KIX binds to purified Pdr1p and that this interaction is further enhanced by xenobiotics (Fig. 2d).

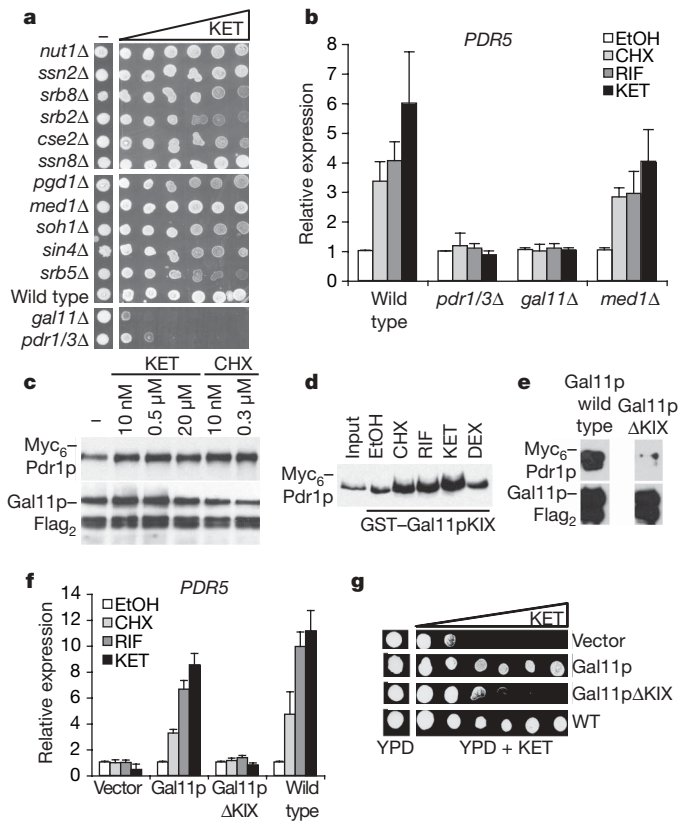


**Figure 2 | Requirement for the Gal11p Mediator subunit and its KIX domain in Pdr1p/Pdr3p-dependent transcription of target genes and MDR.**

**a**, Growth of yeast cells on 1% yeast extract, 2% peptone and 2% dextrose (YPD) with increasing concentrations of ketoconazole reveals a specific requirement for Gal11p for ketoconazole resistance; -, yeasts growing on YPD without ketoconazole. **b**, Gal11p is required for Pdr1p/Pdr3p-mediated and xenobiotic-dependent transcription of the *PDR5* gene. Deletion of *PDR1/3* was used as positive control. Real-time quantitative RT-PCR reactions were performed in triplicate. Mean values are shown; error bars, s.d. **c**, Co-immunoprecipitation shows the interaction between Myc<sub>6</sub>-Pdr1p and Gal11p-Flag<sub>2</sub> in the absence and presence of different concentrations of ketoconazole and cycloheximide. Anti-Flag antibodies were used for immunoprecipitation, with IgG as negative control (no significant binding; data not shown). Anti-Myc (upper panel) and anti-Flag (lower panel) antibodies were used for immunodetection. There is no significant difference in the input material (not shown). **d**, GST-pull-down analysis demonstrates increased interaction between the GST-Gal11pKIX domain and Myc<sub>6</sub>-Pdr1p in the presence of activating xenobiotics. Bound Myc<sub>6</sub>-Pdr1p was detected by anti-Myc immunoblotting. **e**, Co-immunoprecipitation shows the importance of the Gal11p KIX domain for *in vivo* interaction between Gal11p and Pdr1p. Yeast extracts from cells cultured in the presence of ketoconazole expressing Myc<sub>6</sub>-Pdr1p and either Gal11p-Flag<sub>2</sub> or Gal11pΔKIX-Flag<sub>2</sub> were used for co-immunoprecipitation. Immunoprecipitation used anti-Flag antibodies; immunodetection used anti-Myc (upper panel) or anti-Flag (lower panel) antibodies. **f**, The Gal11p KIX domain is required for xenobiotic-induced transcription of *PDR5*. The *gal11Δ* yeast strain was reconstituted with plasmids expressing full-length Gal11p, or Gal11p lacking the KIX domain (amino acids 1–100), or with vector control. Wild-type yeast was used as positive control. Real-time quantitative RT-PCR reactions were performed in triplicate. Mean values are shown; error bars, s.d. **g**, Growth of yeast cells on YPD with increasing concentrations of ketoconazole shows the requirement of the Gal11p KIX domain for ketoconazole resistance. The *gal11Δ* yeast strain was transformed with plasmids harbouring either full-length Gal11p, Gal11p lacking the KIX domain (amino acids 1–100) or vector control. Wild-type yeast was used as positive control. Left panel shows yeast cells grown on YPD without ketoconazole.

Mapping studies revealed that C-terminal Pdr1p sequences containing the activation domain (Pdr1pAD) bind to the Gal11p KIX domain (Supplementary Fig. 6d and data not shown). Interestingly, Pdr1pAD also bound to the CBP and ARC105/MED15 KIX domains (Supplementary Fig. 6d). Consistent with its ability to engage mammalian co-activators, Pdr1pAD fused to Gal4pDBD mediated potent gene activation in human cells (Supplementary Fig. 6e). The Gal11p KIX domain can also interact with the human SREBP-1a activator that we previously showed associates with the ARC105/MED15 and CBP KIX domains (Supplementary Fig. 6b, d)<sup>31,36</sup>. In contrast, the CBP/p300 KIX-binding activators CREB and c-Myb cannot interact with the Gal11p KIX domain, nor with the human ARC105/MED15 KIX domain (Supplementary Fig. 4d)<sup>31,37,38</sup>. These results indicate that the putative Gal11p KIX domain is a specific target only for certain activators, and functionally behaves more like the human ARC105/MED15 KIX domain than the CBP KIX domain, in keeping with the fact that both ARC105/MED15 and Gal11p are components of the Mediator family of co-activators. Our studies also revealed the functional importance of the Gal11p KIX domain for Pdr1p/Pdr3p gene activation and MDR *in vivo*. Deletion of the Gal11p KIX domain strongly decreased interaction of Gal11p with Pdr1p in co-immunoprecipitation experiments (Fig. 2e). Moreover, exogenous expression of wild-type Gal11p, but not KIX-deleted Gal11p, can rescue both xenobiotic-dependent activation of Pdr1p/Pdr3p target genes and resistance to ketoconazole in yeast deleted for *GAL11* (Fig. 2f, g and data not shown).

To provide molecular details that could yield further insights into the gene activation mechanism by Pdr1p, we have determined the solution structure of the Gal11p Pdr1p-binding domain by NMR. The high-resolution structure reveals a three-helix bundle fold with marked similarity to the human ARC105/MED15 and mouse CBP KIX domains (Fig. 3a, b)<sup>31,35</sup>. Like the mammalian KIX domains, the three helices in the Gal11p KIX domain pack an extensively hydrophobic core (Supplementary Fig. 7c). In the ARC105/MED15 and CBP KIX structures, hydrophobic patches on the surface of the KIX domains mediate interactions with several activators (Supplementary Fig. 9)<sup>31,35,38</sup>. We show here by chemical shift analysis that peptides containing the C-terminal 12 and 34 amino acids of the Pdr1pAD also interact with amino acids within a large hydrophobic groove contributed by all three helices, including L25, Q26, M29, I31, L34, A42, I47, N51, F52, A55, V74, A75 and V76 (Fig. 3c and Supplementary Figs 7–10). Binding studies of Pdr1p with point-mutated Gal11p KIX proteins in the presence of ketoconazole also revealed several KIX amino acids as being important for Pdr1p binding, consistent with the NMR data (Fig. 3c–e). NMR showed that yeast Pdr1pAD-34 can also interact with the human ARC105/MED15 KIX domain, consistent with the binding of a larger Pdr1pAD fragment (Supplementary Figs 6d and 10a). Analysis by chemical shift perturbation revealed that the Pdr1p activation domain interaction surface on the Gal11p KIX domain substantially overlaps with that of the human SREBP-1a activation domain (Supplementary Fig. 10d). These results suggest similarities in the way activators target orthologous KIX domains. However, there are also significant differences in the way Pdr1p and SREBP-1a engage their cognate KIX domains (Supplementary Fig. 9). These results agree with earlier observations that different activation domains (for example CREB pKID, c-Myb and MLL) bind both overlapping and distinct epitopes on the human ARC105/MED15 and mouse CBP KIX domains (Supplementary Fig. 9)<sup>31,35,38–43</sup>. Thus, although the structure of the KIX domain is conserved between mammals and yeast, a variety of interfaces on KIX domains are used to accommodate various activation domains. Taken together, our findings reveal that the activator-binding domain in Gal11p indeed folds into a functionally conserved KIX domain; they also pinpoint key residues in the Gal11p KIX domain involved in binding to the Pdr1p activation domain.

### Conservation of xenobiotic gene regulation in *C. glabrata*

Having dissected the molecular mechanisms underpinning the xenobiotic gene regulatory network controlling MDR in the non-pathogenic yeast *S. cerevisiae*, we next determined the potential clinical relevance of our findings for pathogenic fungi. *C. glabrata* is the second most common cause of invasive candidiasis, and has been reported to exhibit intrinsic MDR, in particular to azoles<sup>3,44,45</sup>. *C. glabrata* harbours a highly conserved Pdr1p orthologue that also regulates drug efflux pumps in response to xenobiotics<sup>22,23</sup>. Based on our results with Pdr1p/Pdr3p in *S. cerevisiae*, we hypothesized that CgPdr1p might also directly bind to azoles and other xenobiotics to promote gene expression and MDR in *C. glabrata*.

Expression of the *C. glabrata* drug efflux pump gene *CDR2* is stimulated by xenobiotics in a CgPdr1p-dependent manner, and CgPdr1p is required for the intrinsically high azole resistance of *C. glabrata* (Fig. 4a, b and Supplementary Fig. 11a)<sup>22,23</sup>. We performed complementation experiments in *PDR1/3*-deleted *S. cerevisiae* to test whether expression of CgPdr1p in this strain could functionally substitute for *S. cerevisiae* Pdr1p/Pdr3p. Indeed, CgPdr1p expression rescued both xenobiotic-dependent gene activation and MDR to a similar extent as the expression of ScPdr1p, establishing the functional similarity of these transcription factors (Fig. 4c and data not shown). Importantly, like its *S. cerevisiae* orthologues, CgPdr1p binds directly to radiolabelled ketoconazole, indicating that CgPdr1p also acts by a direct effector mechanism akin to nuclear receptor signalling (Fig. 4d).

Next, we examined the co-activator requirements for xenobiotic-dependent gene activation and MDR in *C. glabrata*. Interestingly, *C. glabrata* harbours two distinct genes with significant sequence

similarity to the *S. cerevisiae* *GAL11* gene (termed CgGAL11A and CgGAL11B here; Supplementary Fig. 11b). Deletion of the CgGAL11A gene strongly decreased xenobiotic-dependent activation of CgCDR2, similar to the effects of deleting CgPDR1, whereas deletion of the CgGAL11B gene had no effect on CgCDR2 expression (Fig. 4a). CgGAL11A deletion also abrogated MDR, causing markedly increased sensitivity to azoles such as ketoconazole and fluconazole, as well as to cycloheximide, as revealed by growth assays (Fig. 4b and data not shown). The CgGAL11A/B double-deletion strain also performed like the CgGAL11A deletion strain (Fig. 4a, b); these data suggest that CgGal11Ap is functionally more important in CgPdr1p xenobiotic-dependent gene activation than CgGal11Bp. Consistent with this notion, a CgPdr1p activation domain fragment interacts better with the CgGal11Ap KIX domain than with the CgGal11Bp KIX domain (Supplementary Fig. 11c).

Non-mammalian hosts, such as the nematode *Caenorhabditis elegans*, have recently been shown to provide powerful and facile model systems to investigate fungal pathogenicity, MDR mechanisms, host response pathways and to identify novel antifungals<sup>46,47</sup>. Infection of *C. elegans* with *C. glabrata* and other *Candida* species results in the death of most nematodes within six days, even in the presence of the antifungal fluconazole (Fig. 4e)<sup>46</sup>. The deletion of CgPDR1, CgGAL11A, CgGAL11B or CgMED1 had little effect on the pathogenicity of *C. glabrata* in this model organism in the absence of antifungals (data not shown). By contrast, in the presence of fluconazole, we observed that nematodes infected with the Cgpd1 and Cggal11A deletion strains exhibited significantly increased survival (Fig. 4e). *C. elegans* infected with the Cggal11B or Cgmed1 deletion strains showed little difference in survival rates in the presence of

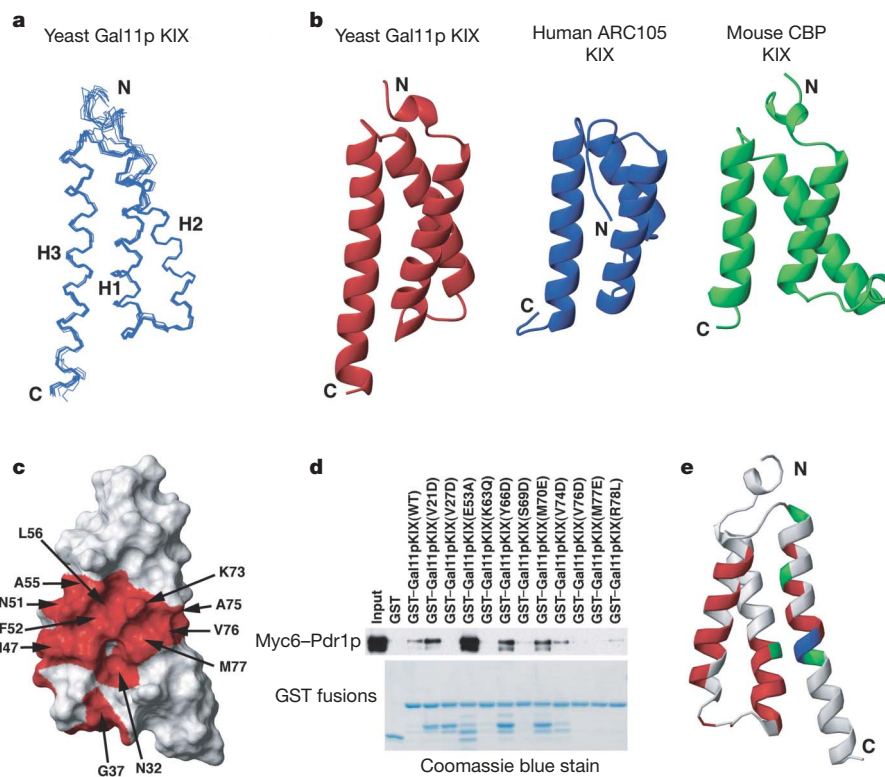


**Figure 3 | Structure of the Gal11p KIX domain and structural/mutational analysis of the Pdr1pAD-Gal11p KIX interface.** **a**, Representation showing the ten lowest energy solution structures of the Gal11p KIX domain. **b**, Ribbon diagram of the mean solution structures of yeast Gal11p, human ARC105/MED15 and mouse CBP KIX domains. **c**, Surface representation of Gal11p KIX with the Pdr1pAD-12 interaction surface (molar ratio 5:1 Gal11p KIX:Pdr1pAD-12) coloured red. The residues shown in red correspond to a chemical shift change of more than 0.02 p.p.m. **d**, Binding of Myc<sub>6</sub>-Pdr1p to point-mutated GST-Gal11p KIX domain fusion proteins in

a GST-pull-down assay. Top panel, Myc<sub>6</sub>-Pdr1p binding as detected by anti-Myc immunoblotting. Bottom panel, GST-Gal11p KIX fusion proteins as detected by Coomassie blue staining. **e**, Ribbon representation of Gal11p KIX where the residues shown in red correspond to a chemical shift change of more than 0.02 p.p.m. upon addition of Pdr1pAD-12 (molar ratio of 5:1 Gal11p KIX:Pdr1pAD-12). Residues whose mutation disrupts binding to Myc<sub>6</sub>-Pdr1p are shown in green; those in blue represent the residues implicated in Pdr1p binding by NMR and mutational studies.

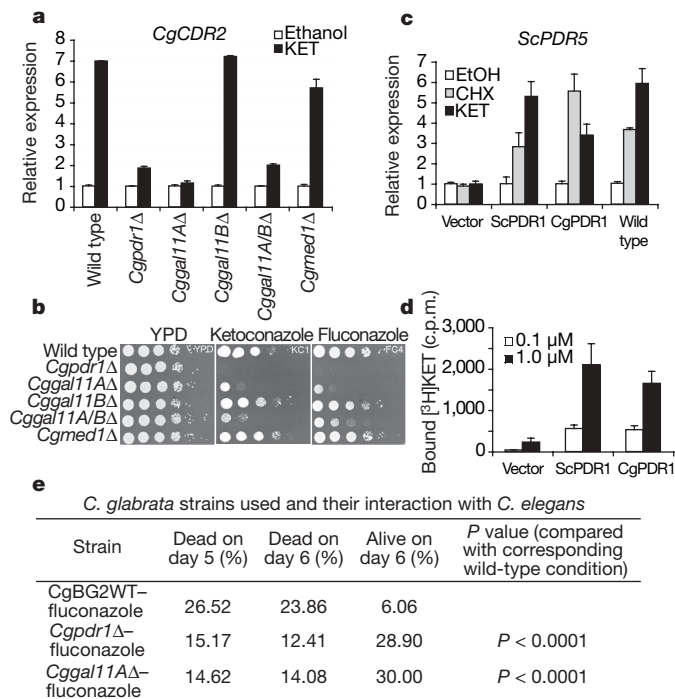


**Figure 4 | Dissection of the molecular mechanism of drug resistance in *C. glabrata*.** **a**, *CgPdr1p* and *CgGal11Ap* are required for ketoconazole-induced transcription of *CgCDR2*. Wild-type and *Cgmed1Δ* strains were used as controls. Real-time quantitative RT-PCR reactions were performed in triplicate. Mean values are shown; error bars, s.d. **b**, Growth of wild-type or mutant *C. glabrata* cells on YPD containing either ethanol vehicle (YPD), ketoconazole (1 μg ml<sup>-1</sup>; KC1) or fluconazole (4 μg ml<sup>-1</sup>; FC4) shows that *CgPdr1p* and *CgGal11Ap* are required for azole resistance in *C. glabrata*. **c**, *CgPdr1p* can functionally complement *ScPdr1p/Pdr3p* for drug-induced *PDR5* transcription. *S. cerevisiae pdr1/3Δ* double-deletion mutant strains transformed with plasmids harbouring either *ScPDR1* or *CgPDR1* complementary DNA (cDNA) or vector were used for this assay. Real-time quantitative RT-PCR reactions were performed in triplicate. Mean values are shown; error bars, s.d. **d**, Binding of [<sup>3</sup>H]KET with *CgPdr1p*. Beads with immunopurified Myc<sub>6</sub>-*CgPdr1p* or Myc<sub>6</sub>-*ScPdr1p* were used for binding assays. Mean values from triplicate experiments are shown; error bars, s.d. **e**, Effect of fluconazole on killing of *C. elegans* by wild-type or mutant strains of *C. glabrata* on days 5 and 6 (120 and 144 h). Fluconazole increased the lifespan of nematodes when the *CgPDR1* and *CgGAL11A* genes were deleted in *C. glabrata*. *P* values were calculated based on the entire 6-day experiment, with log-rank and Wilcoxon tests performed by STATA 6 statistical software (Stata).

fluconazole, similar to wild-type *C. glabrata* (data not shown). These results are consistent with the *in vitro* findings and demonstrate a critical role for the functional interaction of *CgPdr1p* and *CgGal11Ap* in *C. glabrata* MDR *in vivo* in a fungal pathogenesis model.

## Discussion

We have found that fungi harbour sensor/effector regulatory mechanisms governing detoxification response that exhibit intriguing functional similarities to vertebrate nuclear xenobiotic receptors. *Pdr1p* orthologues and *PXR* both bind directly to structurally unrelated xenobiotics and drugs. As a result, they activate the expression of genes encoding ATP-dependent drug efflux pumps (for example P-glycoprotein/MDR1 orthologues) (Supplementary Fig. 1)<sup>24</sup>. Bioinformatics studies based on the conservation of the zinc finger DNA-binding domain and the ligand-binding domain have shown that nuclear receptors first arose during metazoan evolution<sup>48</sup>. Our results revealing functional similarities of fungal *Pdr1p* orthologues and vertebrate *PXR* do not constitute proof of evolutionary orthology. However, taken together with a recent study showing that

the yeast zinc-cluster family member *Oaf1p* may function similarly to the vertebrate *PPARα* nuclear receptor<sup>49</sup>, they suggest that further studies of mechanistic analogies (and possible evolutionary relationships) between fungal zinc-cluster transcription factors and metazoan nuclear receptors are warranted.

We have shown here that fungal *Pdr1p* orthologues interact physically and functionally with the *Gal11p/MED15* subunit of the Mediator. Our data revealing that *Gal11p* harbours an activator-binding domain with marked structural similarity to KIX domains present in metazoan co-activators, indicate strong evolutionary conservation, which implies critical functionality. Interestingly, a recent study showed that the *C. elegans* nuclear receptor *NHR-49* interacts with the KIX-containing *Gal11p* orthologue *MDT-15* and requires *MDT-15* for activation of fatty-acid metabolism genes<sup>50</sup>. This raises the question of whether other metazoan nuclear receptors also use the *ARC105/MED15* subunit as a transducer of gene-activating signals. The targeting of *ARC105/MED15* orthologues in fungi and metazoans might thus represent an ancient mechanism of activation by ligand-dependent transcription factors.

The elucidation of the molecular mechanism of xenobiotic-dependent regulation of MDR by *CgPdr1p* in *C. glabrata* should provide novel targets for the development of 'co-therapeutics' that augment standard antifungal therapies by directly interfering with the mechanistic underpinnings of antifungal-induced MDR (Supplementary Fig. 1). For example, small-molecule antagonists might be identified that lock *Pdr1p* orthologues in an inactive conformation, thereby preventing activation of the efflux pump genes and resulting in sensitization to standard antifungal therapy. Alternatively, the highly hydrophobic groove in the *Gal11p* KIX domain that provides the *Pdr1p* AD docking site might serve as a promising therapeutic target. Our findings should also provide the foundation for studies investigating whether similar regulatory mechanisms govern MDR in other clinically significant pathogenic fungi, such as *Candida albicans*.

## METHODS SUMMARY

Details of plasmids, primers, fungal strains, xenobiotic treatment, quantitative real-time polymerase chain reaction with reverse transcription (qRT-PCR), β-galactosidase assay, drug sensitivity assays, immunoprecipitation and immunoblotting, chromatin immunoprecipitation, drug binding and cold competition assays, glutathione S-transferase (GST) fusion-protein generation and pulldown assays, *C. elegans* fungal killing assays and structural analysis by NMR are given in Supplementary Information.

**Full Methods** and any associated references are available in the online version of the paper at [www.nature.com/nature](http://www.nature.com/nature).

Received 19 October 2007; accepted 5 February 2008.

- Richardson, M. D. Changing patterns and trends in systemic fungal infections. *J. Antimicrob. Chemother.* **56**, i5–i11 (2005).
- Aperis, G., Myriounis, N., Spanakis, E. K. & Mylonakis, E. Developments in the treatment of candidiasis: more choices and new challenges. *Expert Opin. Investig. Drugs* **15**, 1319–1336 (2006).
- Pfaller, M. A. & Diekema, D. J. Epidemiology of invasive candidiasis: a persistent public health problem. *Clin. Microbiol. Rev.* **20**, 133–163 (2007).
- Wisplinghoff, H. et al. Nosocomial bloodstream infections in US hospitals: analysis of 24,179 cases from a prospective nationwide surveillance study. *Clin. Infect. Dis.* **39**, 309–317 (2004).
- Klepser, M. E. *Candida* resistance and its clinical relevance. *Pharmacotherapy* **26**, 685–755 (2006).
- Sipos, G. & Kuchler, K. Fungal ATP-binding cassette (ABC) transporters in drug resistance & detoxification. *Curr. Drug Targets* **7**, 471–481 (2006).
- Balzi, E. et al. The multidrug resistance gene *PDR1* from *Saccharomyces cerevisiae*. *J. Biol. Chem.* **262**, 16871–16879 (1987).
- Meyers, S. et al. Interaction of the yeast pleiotropic drug resistance genes *PDR1* and *PDR5*. *Curr. Genet.* **21**, 431–436 (1992).
- Balzi, E. et al. *PDR5*, a novel yeast multidrug resistance conferring transporter controlled by the transcription regulator *PDR1*. *J. Biol. Chem.* **269**, 2206–2214 (1994).
- Katzmann, D. J. et al. Transcriptional control of the yeast *PDR5* gene by the *PDR3* gene product. *Mol. Cell. Biol.* **14**, 4653–4661 (1994).

11. Delaveau, T. *et al.* PDR3, a new yeast regulatory gene, is homologous to PDR1 and controls the multidrug resistance phenomenon. *Mol. Gen. Genet.* **244**, 501–511 (1994).
12. Decottignies, A. *et al.* Identification and characterization of SNQ2, a new multidrug ATP binding cassette transporter of the yeast plasma membrane. *J. Biol. Chem.* **270**, 18150–18157 (1995).
13. Katzmann, D. J. *et al.* Expression of an ATP-binding cassette transporter-encoding gene (YOR1) is required for oligomycin resistance in *Saccharomyces cerevisiae*. *Mol. Cell. Biol.* **15**, 6875–6883 (1995).
14. van den Hazel, H. B. *et al.* PDR16 and PDR17, two homologous genes of *Saccharomyces cerevisiae*, affect lipid biosynthesis and resistance to multiple drugs. *J. Biol. Chem.* **274**, 1934–1941 (1999).
15. Moye-Rowley, W. S. Transcriptional control of multidrug resistance in the yeast *Saccharomyces*. *Prog. Nucleic Acid Res. Mol. Biol.* **73**, 251–279 (2003).
16. Mamnun, Y. M., Schuller, C. & Kuchler, K. Expression regulation of the yeast PDR5 ATP-binding cassette (ABC) transporter suggests a role in cellular detoxification during the exponential growth phase. *FEBS Lett.* **559**, 111–117 (2004).
17. Gao, C., Wang, L., Milgrom, E. & Shen, W. C. On the mechanism of constitutive Pdr1 activator-mediated PDR5 transcription in *Saccharomyces cerevisiae*: evidence for enhanced recruitment of coactivators and altered nucleosome structures. *J. Biol. Chem.* **279**, 42677–42686 (2004).
18. Lucau-Danila, A. *et al.* Early expression of yeast genes affected by chemical stress. *Mol. Cell. Biol.* **25**, 1860–1868 (2005).
19. Alenquer, M., Tenreiro, S. & Sa-Correia, I. Adaptive response to the antimalarial drug artesunate in yeast involves Pdr1p/Pdr3p-mediated transcriptional activation of the resistance determinants TPO1 and PDR5. *FEMS Yeast Res.* **6**, 1130–1139 (2006).
20. Fardeau, V. *et al.* The central role of PDR1 in the foundation of yeast drug resistance. *J. Biol. Chem.* **282**, 5063–5074 (2007).
21. Vermitsky, J. P. & Edlind, T. D. Azole resistance in *Candida glabrata*: coordinate upregulation of multidrug transporters and evidence for a Pdr1-like transcription factor. *Antimicrob. Agents Chemother.* **48**, 3773–3781 (2004).
22. Tsai, H. F., Krol, A. A., Sarti, K. E. & Bennett, J. E. *Candida glabrata* PDR1, a transcriptional regulator of a pleiotropic drug resistance network, mediates azole resistance in clinical isolates and petite mutants. *Antimicrob. Agents Chemother.* **50**, 1384–1392 (2006).
23. Vermitsky, J. P. *et al.* Pdr1 regulates multidrug resistance in *Candida glabrata*: gene disruption and genome-wide expression studies. *Mol. Microbiol.* **61**, 704–722 (2006).
24. Kliever, S. A., Goodwin, B. & Willson, T. M. The nuclear pregnane X receptor: a key regulator of xenobiotic metabolism. *Endocr. Rev.* **23**, 687–702 (2002).
25. Willson, T. M. & Kliever, S. A. PXR, CAR and drug metabolism. *Nature Rev. Drug Discov.* **1**, 259–266 (2002).
26. Näär, A. M., Lemon, B. D. & Tjian, R. Transcriptional coactivator complexes. *Annu. Rev. Biochem.* **70**, 475–501 (2001).
27. Kornberg, R. D. Mediator and the mechanism of transcriptional activation. *Trends Biochem. Sci.* **30**, 235–239 (2005).
28. Kean, L. S. *et al.* Plasma membrane translocation of fluorescently-labeled phosphatidylethanolamine is controlled by transcription regulators, PDR1 and PDR3. *J. Cell Biol.* **138**, 255–270 (1997).
29. Gulshan, K., Rovinsky, S. A., Coleman, S. T. & Moye-Rowley, W. S. Oxidant-specific folding of Yap1p regulates both transcriptional activation and nuclear localization. *J. Biol. Chem.* **280**, 40524–40533 (2005).
30. Novatchkova, M. & Eisenhaber, F. Linking transcriptional mediators via the GACKIX domain super family. *Curr. Biol.* **14**, R54–R55 (2004).
31. Yang, F. *et al.* An ARC/Mediator subunit required for SREBP control of cholesterol and lipid homeostasis. *Nature* **442**, 700–704 (2006).
32. Goodman, R. H. & Smolik, S. CBP/p300 in cell growth, transformation, and development. *Genes Dev.* **14**, 1553–1577 (2000).
33. Kasper, L. H. *et al.* A transcription-factor-binding surface of coactivator p300 is required for haematopoiesis. *Nature* **419**, 738–743 (2002).
34. Kasper, L. H. *et al.* Conditional knockout mice reveal distinct functions for the global transcriptional coactivators CBP and p300 in T-cell development. *Mol. Cell. Biol.* **26**, 789–809 (2006).
35. Radhakrishnan, I. *et al.* Solution structure of the KIX domain of CBP bound to the transactivation domain of CREB: a model for activator:coactivator interactions. *Cell* **91**, 741–752 (1997).
36. Näär, A. M. *et al.* Chromatin, TAFs, and a novel multiprotein coactivator are required for synergistic activation by Sp1 and SREBP-1a in vitro. *Genes Dev.* **12**, 3020–3031 (1998).
37. Dai, P. *et al.* CBP as a transcriptional coactivator of c-Myb. *Genes Dev.* **10**, 528–540 (1996).
38. Zor, T., De Guzman, R. N., Dyson, H. J. & Wright, P. E. Solution structure of the KIX domain of CBP bound to the transactivation domain of c-Myb. *J. Mol. Biol.* **337**, 521–534 (2004).
39. De Guzman, R. N., Goto, N. K., Dyson, H. J. & Wright, P. E. Structural basis for cooperative transcription factor binding to the CBP coactivator. *J. Mol. Biol.* **355**, 1005–1013 (2006).
40. Goto, N. K. *et al.* Cooperativity in transcription factor binding to the coactivator CREB-binding protein (CBP). The mixed lineage leukemia protein (MLL) activation domain binds to an allosteric site on the KIX domain. *J. Biol. Chem.* **277**, 43168–43174 (2002).
41. Parker, D. *et al.* Analysis of an activator:coactivator complex reveals an essential role for secondary structure in transcriptional activation. *Mol. Cell* **2**, 353–359 (1998).
42. Parker, D. *et al.* Role of secondary structure in discrimination between constitutive and inducible activators. *Mol. Cell. Biol.* **19**, 5601–5607 (1999).
43. Radhakrishnan, I. *et al.* Structural analyses of CREB–CBP transcriptional activator–coactivator complexes by NMR spectroscopy: implications for mapping the boundaries of structural domains. *J. Mol. Biol.* **287**, 859–865 (1999).
44. Prasad, R., Gaur, N. A., Gaur, M. & Komath, S. S. Efflux pumps in drug resistance of *Candida*. *Infect. Disord. Drug Targets* **6**, 69–83 (2006).
45. Pfaller, M. A. *et al.* Results from the ARTEMIS DISK Global Antifungal Surveillance study, 1997 to 2005: an 8.5-year analysis of susceptibilities of *Candida* species and other yeast species to fluconazole and voriconazole determined by CLSI standardized disk diffusion testing. *J. Clin. Microbiol.* **45**, 1735–1745 (2007).
46. Breger, J. *et al.* Antifungal chemical compounds identified using a *C. elegans* pathogenicity assay. *PLoS Pathogens* **3**, e18 (2007).
47. Mylonakis, E. & Aballay, A. Worms and flies as genetically tractable animal models to study host–pathogen interactions. *Infect. Immun.* **73**, 3833–3841 (2005).
48. Bertrand, S. *et al.* Evolutionary genomics of nuclear receptors: from twenty-five ancestral genes to derived endocrine systems. *Mol. Biol. Evol.* **21**, 1923–1937 (2004).
49. Phelps, C. *et al.* Fungi and animals may share a common ancestor to nuclear receptors. *Proc. Natl Acad. Sci. USA* **103**, 7077–7081 (2006).
50. Taubert, S., Van Gilst, M. R., Hansen, M. & Yamamoto, K. R. A Mediator subunit, MDT-15, integrates regulation of fatty acid metabolism by NHR-49-dependent and -independent pathways in *C. elegans*. *Genes Dev.* **20**, 1137–1149 (2006).

**Supplementary Information** is linked to the online version of the paper at [www.nature.com/nature](http://www.nature.com/nature).

**Acknowledgements** We thank C. Wivagg and M. Franzmann for their help with the NMR assignment and fluorescence studies; and N. Dyson, S. Buratowski, A. Walker and H. Najafi-Shoushtari for comments on the manuscript. We were unable to cite many original papers owing to space constraints. This work was supported by grants from the National Institutes of Health: GM071449 (A.M.N.), CA127990 (G.W./A.M.N.), A1046223 (B.P.C.), GM49825 (W.S.M.-R.) and GM30186 (K.S.). The NMR facility used for this research was supported by grants GM47467 and EB2026. J.K.T. was supported by a fellowship from the MGH Fund for Medical Discovery.

**Author Information** The NMR structure is deposited in the Protein Data Bank under accession number 2k0n. Reprints and permissions information is available at [www.nature.com/reprints](http://www.nature.com/reprints). Correspondence and requests for materials should be addressed to A.M.N. ([naar@helix.mgh.harvard.edu](mailto:naar@helix.mgh.harvard.edu)).

## METHODS

**Media and chemicals.** All bacteria were routinely grown in Luria-Bertani broth medium with required antibiotics. *S. cerevisiae* cells were grown either in YPD or in synthetic defined medium as required. For culturing *C. glabrata*, we used synthetic complete medium<sup>51</sup>. Unless specified, all chemicals and drugs were purchased from Sigma. Anti-HA (F-7) and anti-c-Myc (9E10) antibodies were obtained from Santa Cruz Biotechnology, whereas anti-Flag M2 antibody was purchased from Sigma. Glutathione-, Protein A- and Protein G-Sepharose beads were obtained from Amersham Pharmacia Biotech.

**Strains and plasmids.** *Escherichia coli* strains DH5 $\alpha$  and DH10 were used for all plasmid maintenance and construction. Yeast strains used in this study are listed in Supplementary Table 1. Yeast transformation was performed using a standard LiCl method<sup>52</sup>. All *C. glabrata* deletion strains were derived from our wild-type laboratory strain BG2 or from a *ura3* derivative of BG2, BG14<sup>53</sup>. Gal4pDBD-Pdr1p or GST-Pdr1p fusion constructs were generated by cloning PCR fragments of *PDR1* of specified size and region, into pGBKT7 (Clontech) or pGEX2-TKN in frame with Gal4pDBD or GST, respectively, using *NcoI* and *NotI* restriction sites. Yeast constructs expressing C-terminal Flag-tagged full-length Gal11p (Gal11p-Flag<sub>2</sub>) or Gal11p with deletion of the KIX domain (amino acids 1–100) (Gal11p $\Delta$ KIX-Flag<sub>2</sub>), and N-terminal Myc-tagged full-length wild-type Pdr1p (Myc<sub>6</sub>-Pdr1pwt), were generated by subcloning the PCR products into the plasmids pCU416 and pCU315, respectively. DNA fragments encoding CgGal11p KIX domains (CgGal11Ap (amino acids 1–86) and CgGal11Bp (amino acids 1–82)) were amplified by PCR from genomic DNA and subcloned into pGEX-2TKN. Point-mutated pGEX-2TKN-Gal11pKIX (amino acids 1–100) plasmids were produced using the Quickchange XL site-directed mutagenesis kit (Stratagene). The mammalian constructs expressing HA-Gal4DBD activation domains of ScPdr1p, ScPdr3p, ScGal4p and CgPdr1p were generated by subcloning the PCR products into pcDNA3-HA-Gal4DBD using *Bam*HI and *Eco*RI sites. All plasmids were confirmed by DNA sequencing.

***C. glabrata* strain construction.** The DNA sequences of the *C. glabrata* genes *PDR1* (CAGL0A00451g), *GAL11A* (CAGL0H06215g), *GAL11B* (CAGL0F00803g) and *MED1* (CAGL0D01386g) were taken from the Génolevures website (<http://cbi.labri.fr/Genolevures/blast.php>) and used to design primers for construction of disruption constructs and restoration constructs. Disruption constructs for *C. glabrata* genes are derived from pAP599 in which an *hph* expression cassette (from 5' to 3', a 500 base pair (bp) *S. cerevisiae* *PGK1* promoter followed by *Klebsiella pneumoniae hph* coding sequences (CDSs) and a 400 bp *S. cerevisiae* *HIS3* 3' untranslated region (UTR)) that confers hygromycin B resistance (Hyg<sup>R</sup>) is immediately flanked by *S. cerevisiae* *FRT* sites and then by multiple cloning sites (MCSs). A 0.5–1 kilobase (kb) 5' UTR and a 0.5–1 kb 3' UTR fragment of the target *C. glabrata* gene were amplified from BG2 genomic DNA by PCR and individually subcloned into pAP599. The accuracy of the cloned fragments was verified by DNA sequencing. The disruption construct containing the target gene 5' and 3' UTRs flanking the *hph* expression cassette was released from the gene disruption plasmid by restriction digest and used to transform BG14 to Hyg<sup>R</sup>. The correct gene disruption was confirmed by PCR amplification. The *hph* expression cassette was then removed by transformation of the strains with a self-replicating plasmid, pRD16, that carries an expression cassette for *S. cerevisiae* *FLP1* (a 2.5 kb *C. glabrata* *EPA1* promoter followed by the *S. cerevisiae* *FLP1* coding region). The Flp1 recombinase recognizes the *FRT* sites immediately flanking the integrated *hph* expression cassette and releases the cassette. pRD16 was subsequently lost by streaking cells on plates containing 5-FOA, which selects against *URA3*. The resulting strains (BG1710–1713) were then restored to Ura<sup>+</sup> by transforming yeast cells with *PstI*-digested pBC34.1, which carries an intact *C. glabrata* *URA3* on a 4.1 kb *PstI* fragment to generate strains 1718–1721. *gal11A gal11B* double mutant was generated by disruption of *GAL11B* in strain BG1710.

**Treatment of yeast cultures with different xenobiotics.** Yeast cultures were grown overnight with agitation in YPD at 30 °C. The next day, cells were pelleted and washed twice with sterilized MilliQ purified (Millipore) water. Cells were then resuspended in 1% yeast extract and 2% peptone (YP) to an optical density (OD<sub>600</sub>) of 0.8, grown for another 16 h at 30 °C, then treated with different drugs for 20 min for quantitative RT-PCR, or 5 h for  $\beta$ -galactosidase assay.

**Quantitative real-time RT-PCR.** Total RNA was extracted from 5 ml of yeast culture using the Qiagen RNeasy MiniKit. Two micrograms of total RNA was used to generate cDNA using the First-Strand cDNA Synthesis Kit (GE Healthcare). The cDNA mix was diluted tenfold, and 2  $\mu$ l was used for real-time quantitative PCR with SYBR Green (Applied Biosystems) on an ABI Prism 7900HT Sequence Detection System (Applied Biosystems).

**$\beta$ -Galactosidase assay.** Yeast culture (1.5 ml) was harvested by brief spinning. The pellet was resuspended in 300  $\mu$ l of Z buffer (10 mM Na<sub>2</sub>HPO<sub>4</sub>·7H<sub>2</sub>O, 10 mM NaH<sub>2</sub>PO<sub>4</sub>·H<sub>2</sub>O, 10 mM KCl, 1 mM MgSO<sub>4</sub>·7H<sub>2</sub>O, pH 7.0). One hundred

microlitres of this suspension was transferred to a fresh tube and subjected to three cycles of freeze (30 s in liquid N<sub>2</sub>) and thaw (1 min at 37 °C). After this, 0.7 ml of Z buffer with  $\beta$ -mercaptoethanol (0.27 ml  $\beta$ -mercaptoethanol in 100 ml of Z buffer) was added, immediately followed by addition of 160  $\mu$ l of ONPG solution (4 mg ml<sup>-1</sup> in Z buffer). The tube was kept at 30 °C until yellow colour developed, when 0.4 ml of 1 M Na<sub>2</sub>CO<sub>3</sub> was added to stop the reaction. The cell debris was pelleted by centrifugation, and the supernatant was used to measure OD<sub>420</sub>. All the readings were normalized to the concentration of protein (as determined by Bradford). All experiments were performed with three independent replicates.

**Drug sensitivity assays.** Fresh *S. cerevisiae* colonies were inoculated in 5 ml of YPD or SD selection medium, and grown overnight at 30 °C. The cells were diluted to an OD<sub>600</sub> of 0.2, and 2  $\mu$ l was spotted on solid medium containing an increasing gradient of drugs (ketoconazole, cycloheximide or 4-NQO) in the agar. The plates were incubated at 30 °C for 2–3 days. Susceptibility of the *C. glabrata* mutants was tested by spotting serial dilutions of cells onto YPD agar plates supplemented with fluconazole or ketoconazole. The yeast strains were grown overnight at 30 °C in YPD liquid medium. Cells were diluted to an OD<sub>600</sub> of 2.0 in PBS, and 4  $\mu$ l of the cell suspension and tenfold serial dilutions of the cells were spotted onto plates. Growth was assessed after 1 day of incubation at 30 °C.

**Immunoprecipitation and immunoblotting.** For co-immunoprecipitation, yeast cells were transformed with Myc<sub>6</sub>-Pdr1pwt and Gal11p-Flag<sub>2</sub> (or Gal11p $\Delta$ KIX-Flag<sub>2</sub>). Cells were washed with 1  $\times$  PBS after overnight culture in YPD medium, and then cultured in YP for another 24 h. Cells were then treated with different concentrations of ketoconazole and cycloheximide (or ethanol for vehicle controls) for 1 h. Yeast cell lysates were extracted in immunoprecipitation buffer (50 mM Tris-HCl, pH 8.0, 140 mM NaCl, 0.1 mM EDTA, 10% glycerol, 0.02% NP-40, 1 mM DTT, 0.25 mM PMSF, 1 mM benzamide, 0.5 mg ml<sup>-1</sup> aprotinin and Protease Inhibitor Cocktail (Complete, Roche)), with or without xenobiotics by vortexing in the presence of glass beads. The Flag-tagged proteins were then immunoprecipitated by adding anti-Flag M2 antibody-beads (Sigma) and incubating for 3 h with nutating at 4 °C. After washing five times with 1 ml of 0.25 M KCl IP buffer, bound proteins were eluted with 0.1 mg ml<sup>-1</sup> Flag peptide (Sigma). Xenobiotics at the indicated concentrations were present at all steps of the co-immunoprecipitation, including washing. Immunoblotting was performed according to standard protocols. To immunoprecipitate Myc<sub>6</sub>-Pdr1pwt or HA-Pdr1pwt, yeast whole-cell extract (in immunoprecipitation buffer) was incubated with anti-Myc (9E10) antibody or anti-HA (F-7) antibody, and 50% mix of Protein A- and G-Sepharose beads (Amersham) at 4 °C for 3 h. Beads were washed with IP buffer five times, and used for drug-binding experiments as outlined below.

**Chromatin immunoprecipitation.** Chromatin immunoprecipitation was performed according to standard procedures<sup>54</sup>. Briefly, yeast cells were grown to an OD<sub>600</sub> of 0.8 before fixing with 1% formaldehyde for 20 min. The cells were washed with Tris-buffered saline (20 mM Tris-HCl, pH 7.5, and 150 mM NaCl), and resuspended in 1 ml of FA lysis buffer (50 mM HEPES, pH 7.5, 150 mM NaCl, 1 mM EDTA, 1% Triton X-100, 0.1% sodium deoxycholate and 0.1% SDS). Cells were lysed using soda lime 0.5 mm glass beads and Beadbeater (BioSpec Products). The glass beads were then removed and the cell debris with chromatin was subjected to sonication (550 sonic dismembrator, Fisher) two times for 30 s each, separated by incubation for 2 min on ice. The soluble chromatin was collected in a fresh tube. Chromatin (300  $\mu$ l) was used for immunoprecipitation with anti-HA Ab and Protein A-Sepharose beads (Amersham), and the immunoprecipitated chromatin was eluted with 200  $\mu$ l of 0.5 mg ml<sup>-1</sup> HA peptide (Sigma) in Tris-buffered saline. Input and immunoprecipitated chromatin were de-crosslinked at 65 °C overnight, and then passed through a Qiagen PCR purification column. The purified DNA was analysed by quantitative PCR in real-time using the ABI Prism 7900HT Sequence Detection System (Applied Biosystems). Relative occupancy values were calculated by determining the apparent immunoprecipitation efficiency and normalized to the level observed at an open reading frame (ORF)-free region from chromosome V.

**Drug-binding and cold competition assay.** Xenobiotic-binding experiments were performed essentially as described<sup>55</sup> with some modifications as explained below. Radiolabelled ketoconazole (KET: [<sup>3</sup>H]G), specific radioactivity 10 Ci mmol<sup>-1</sup>, was purchased from American Radiolabelled Chemicals. Beads with either immunopurified proteins or GST recombinant proteins were incubated with KET ([<sup>3</sup>H]G) in drug-binding buffer (10 mM K<sub>2</sub>HPO<sub>4</sub>, 10 mM KH<sub>2</sub>PO<sub>4</sub>, pH 7.0, 2 mM EDTA, 50 mM NaCl, 1 mM DTT, 0.5 mM CHAPS, 10% glycerol and protease inhibitors) at 4 °C for 3 h with mixing in a volume of 500  $\mu$ l. For cold competition, unlabelled xenobiotics were added to a concentration of 1,000-fold excess of KET. The beads were then washed thrice briefly in 900  $\mu$ l of ice cold drug-binding buffer, carefully removing as much of each wash as

possible. The washed beads were resuspended in 100  $\mu$ l of drug-binding buffer, added to 5 ml of scintillation fluid Aquasol-2 (Perkin Elmer) and mixed briefly by shaking. After 10 min, scintillation counting was performed in an LS6500 Multi-Purpose Scintillation Counter (Beckman Coulter). All experiments were performed with at least three replicates.

**GST pull-down assays.** Recombinant GST-fusion proteins were expressed in *E. coli* (BL21, DE3) and purified using glutathione-Sepharose beads according to standard protocol (Pharmacia). Beads with GST proteins were incubated with either whole-cell lysate or *in vitro* translated protein mix in binding buffer (20 mM Tris-HCl, pH 8.0, 150 mM NaCl, 0.1 mM EDTA, 10% glycerol, 0.05% NP-40, 1 mM DTT, 0.25 mM PMSF, 1 mM benzamide and Protease Inhibitor Cocktail for yeast extracts (Sigma)), for 3 h at 4 °C. The beads were washed five times with wash buffer (20 mM Tris-HCl, pH 8.0, 250 mM KCl, 0.1 mM EDTA, 10% Glycerol, 0.1% NP-40, 1 mM DTT, 0.25 mM PMSF, 1 mM benzamide and Protease Inhibitor Cocktail). The beads were finally washed once with binding buffer. The bound proteins were then eluted with 50  $\mu$ l of 0.3% sarkosyl in binding buffer for 1 h at 4 °C. The eluted proteins were resolved on 10% polyacrylamide gel and detected either by immunoblotting or by autoradiography.

**Large-scale purification and identification of GST-Gal1p KIX-associated proteins in yeast.** Yeast (61) cultured in YPD medium overnight was harvested by centrifugation and washing once with distilled water. The cell pellet was then resuspended in 0.25 volumes of lysis buffer (50 mM Tris-HCl (pH 8.0), 400 mM NaCl, 5 mM MgCl<sub>2</sub>, 1 mM EGTA, 1 mM EDTA, 0.1% NP40, 1 mM DTT, 0.25 mM PMSF, 1 mM benzamide, 0.5 mg ml<sup>-1</sup> aprotinin and Protease Inhibitor Cocktail (Complete, Roche)), and the suspension was quick-frozen in liquid nitrogen. Frozen cells were lysed by grinding with a mortar and pestle together with dry ice. One volume of lysis buffer was added after evaporation with dry ice, and the extract was spun at 4,000g for 10 min. The supernatant was pre-incubated with 200  $\mu$ l glutathione-Sepharose-bound GST for 2 h at 4 °C with rotation, then it was incubated for another 3 h at 4 °C with 200  $\mu$ l glutathione-Sepharose-bound GST-Gal1p KIX (amino acids 1–100). The beads were washed seven times with wash buffer (20 mM Tris-HCl, pH 8.0, 250 mM KCl, 0.1 mM EDTA, 10% glycerol, 0.1% NP-40, 5 mM MgCl<sub>2</sub>, 1 mM EGTA, 1 mM EDTA, 1 mM DTT, 0.25 mM PMSF, 1 mM benzamide and Protease Inhibitor Cocktail). The beads were finally washed once with low salt (150 mM NaCl) wash buffer. The bound proteins were then eluted with 500  $\mu$ l of 0.3% sarkosyl in binding buffer for 1 h at 4 °C and dialysed overnight in 1 l of dialysis buffer (1% SDS, 1 mM  $\beta$ -mercaptoethanol and 1 mM Tris-HCl, pH 8.0). The dialysed eluate was concentrated by dry-ice/ethanol SpeedVac to approximately 80  $\mu$ l. The eluted proteins were resolved on 10% polyacrylamide gel and stained with Coomassie colloidal blue. The specific band at about 120 kDa was excised and subjected to trypsin digestion, followed by liquid chromatography MS/MS (LC-MS/MS) at the Taplin Biological Mass Spectrometry Facility at Harvard Medical School.

***C. elegans* liquid killing assays.** The *C. glabrata* strains and lawns were grown and prepared as described previously<sup>56</sup>. The liquid medium killing assays were conducted as detailed in ref. 56, with a few changes. After the *glp-4;sek-1* worms were incubated at 25 °C for two days, they were washed off the nematode growth medium plates with M9 and transferred to *C. glabrata* lawns formed on Brain-Heart Infusion broth (Difco) agar plates. The worms were incubated on the lawns for 4 h at 25 °C, then washed off the plates with M9 buffer and allowed to crawl on unseeded Brain-Heart Infusion broth plates to remove yeast cells from their cuticles. Approximately 70–80 worms were then picked to wells in a six-well microtitre dish that contained 2 ml of liquid medium of 79% M9 buffer, 20% Brain-Heart Infusion broth, 10  $\mu$ g ml<sup>-1</sup> cholesterol in ethanol, and 90  $\mu$ g ml<sup>-1</sup> kanamycin, with the addition of 0.25% DMSO or 8  $\mu$ g ml<sup>-1</sup> fluconazole. The plates were incubated at 25 °C overnight and then examined at 24 h intervals for survival. Worms were considered dead and removed when they did not respond to being touched by a platinum wire pick. *P* values were calculated based on the entire six-day experiment with the log-rank and Wilcoxon tests performed by STATA 6 statistical software (Stata).

**Structural analysis by NMR.** A pET24b plasmid containing the Gal1p KIX sequence with an N-terminal His<sub>6</sub>-tag followed by a cleavage site for the tobacco etch virus protease was transformed into *E. coli* BL21 (DE3) cells. The cells were grown to an OD<sub>600</sub> of 0.7 at 37 °C and induced for 12–16 h at 25 °C with 1 mM isopropyl  $\beta$ -D-1-thiogalactopyranoside. The cells were lysed by sonication, centrifuged and the supernatant was purified by Ni-NTA resin (Qiagen). The His tag was cleaved off by Tev protease overnight at 4 °C. This sample was further purified by fast protein liquid chromatography using a size exclusion column (Sephadex 75, Pharmacia). All NMR samples were in PBS buffer (10 mM Na<sub>2</sub>HPO<sub>4</sub>, 2 mM K<sub>2</sub>HPO<sub>4</sub>, 137 mM NaCl, 2.7 mM KCl, 1 mM EDTA and

0.01% NaN<sub>3</sub>), pH 6.5, unless otherwise stated. Pdr1pAD-34 was expressed as a GST-fusion tag in *E. coli* BL21 (DE3) cells. The protein was purified as described above with the fusion tag cleaved after Nickel resin purification. <sup>15</sup>N/<sup>13</sup>C-labelled samples of Gal1p KIX and Pdr1pAD-34 were obtained by overexpression of the respective proteins in M9 minimal media enriched with <sup>15</sup>NH<sub>4</sub>Cl and/or [<sup>13</sup>C]glucose. Perdeuterated samples of Gal1p KIX were generated in similar fashion with the protein expressed in M9 minimal media in <sup>2</sup>H<sub>2</sub>O using [<sup>13</sup>C-<sup>2</sup>H]glucose. Pdr1pAD-12 (H<sub>4</sub>N-EDLYSILWSDVY-COOH) and SREBP-1a-26 (H<sub>4</sub>N-EPCDLDAALLTDIEDMLQLINNQDSD-COOH) were purchased as synthetic peptides from Tufts New England Medical Center peptide synthesis facility. Titrations with the peptide were performed in a 'high phosphate buffer' (50 mM Na<sub>2</sub>HPO<sub>4</sub>, 50 mM NaH<sub>2</sub>PO<sub>4</sub>, 2 mM K<sub>2</sub>HPO<sub>4</sub>, 2.7 mM KCl, 1 mM EDTA and 0.01% NaN<sub>3</sub>) to maintain the pH during the course of the titration. For NMR spectroscopy, backbone assignments were mostly obtained by the standard set of triple resonance experiments (HNCA/HNCOCA, HNCACB/CBCACONH, HNCO/HNCACO)<sup>57</sup>. Because the Gal1p KIX exhibited stretches that were difficult to assign, we used a time-shared (HA)CANH/(HN)NCAHA to verify and complete the backbone assignment<sup>58</sup>. The side-chain residues were assigned using HCCONH and CCONH experiments of Gal1p KIX in H<sub>2</sub>O and HCCH-TOSY in <sup>2</sup>H<sub>2</sub>O. <sup>15</sup>N-dispersed heteronuclear single-quantum coherence-nuclear overhauser enhancement spectroscopy (HSQC-NOESY) with a mixing time of 90 ms was recorded to provide distance constraints. All backbone experiments were performed on a Bruker 600 MHz spectrometer equipped with a cryoprobe. The side-chain and NOESY experiments were performed on Bruker 500 MHz and 900 MHz spectrometers, respectively. Cross-saturation experiments were performed using perdeuterated samples of <sup>15</sup>N-enriched Gal1p KIX and unlabelled Pdr1pAD-12. The methyl region (1 p.p.m.) was excited with a wideband uniform rate smooth truncation pulse for 2 s, and this was followed by a standard HSQC experiment. The experiment was performed in an interleaved fashion with irradiation and no irradiation in successive scans. The ratio of intensities between the irradiated HSQC and the non-irradiated HSQC was later analysed<sup>59</sup>. ARC105 KIX was expressed as a GST fusion protein and purified over a glutathione-Sepharose column. ARC105 KIX was cleaved from GST using tobacco etch virus protease. The cleaved protein was further purified by fast protein liquid chromatography using a size exclusion column (Sephadex 75, Pharmacia) in a buffer containing 30 mM NaCl, 5 mM Na<sub>2</sub>HPO<sub>4</sub> and 5 mM KH<sub>2</sub>PO<sub>4</sub> at pH 6.8. For titration experiments, unlabelled Pdr1pAD-34 was purified in the same buffer as mentioned above and added to ARC105 KIX.

For NMR Structure calculations, NMR structure refinement was performed using the program CYANA<sup>60</sup>. Torsion angle constraints (146 constraints) were calculated using the program TALOS<sup>61</sup>. Assignment of the backbone and side-chain resonances was performed using the program CARA. One thousand three hundred and fifty-nine distance restraints were calculated from the <sup>15</sup>N-dispersed NOESY experiments. NOESY cross peaks were integrated using the program PeakInt.

- Sherman, F., Fink, G. R. & Hicks, J. B. *Methods in Yeast Genetics* (Cold Spring Harbor Laboratory, Cold Spring Harbor, New York, 1986).
- Gietz, D., St Jean, A., Woods, R. A. & Schiestl, R. H. Improved method for high efficiency transformation of intact yeast cells. *Nucleic Acids Res.* **20**, 1425 (1992).
- Cormack, B. P. & Falkow, S. Efficient homologous and illegitimate recombination in the opportunistic yeast pathogen *Candida glabrata*. *Genetics* **151**, 979–987 (1999).
- Aparicio, J. G., Viggiani, C. J., Gibson, D. G. & Aparicio, O. M. The Rpd3-Sin3 histone deacetylase regulates replication timing and enables intra-S origin control in *Saccharomyces cerevisiae*. *Mol. Cell. Biol.* **24**, 4769–4780 (2004).
- Kepinski, S. & Leyser, O. The *Arabidopsis* F-box protein TIR1 is an auxin receptor. *Nature* **435**, 446–451 (2005).
- Breger, J. et al. Antifungal chemical compounds identified using a *C. elegans* pathogenicity assay. *PLoS Pathogens* **3**, e18 (2007).
- Ferentz, A. E. & Wagner, G. NMR spectroscopy: a multifaceted approach to macromolecular structure. *Q. Rev. Biophys.* **33**, 29–65 (2000).
- Frueh, D. P., Arthanari, H. & Wagner, G. Unambiguous assignment of NMR protein backbone signals with a time-shared triple-resonance experiment. *J. Biomol. NMR* **33**, 187–196 (2005).
- Takahashi, H. et al. A novel NMR method for determining the interfaces of large protein-protein complexes. *Nature Struct. Mol. Biol.* **7**, 220–223 (2000).
- Guntert, P., Mumenthaler, C. & Wuthrich, K. Torsion angle dynamics for NMR structure calculation with the new program DYANA. *J. Mol. Biol.* **273**, 283–298 (1997).
- Cornilescu, G., Delaglio, F. & Bax, A. Protein backbone angle restraints from searching a database for chemical shift and sequence homology. *J. Biomol. NMR* **13**, 289–302 (1999).